Measuring Glymphatic Flow in Man Using Quantitative Contrast-Enhanced MRI

R. Watts, J.M. Steinklein, L. Waldman, X. Zhou, and C.G. Filippi

ABSTRACT

SUMMARY: On the basis of animal models, glymphatic flow disruption is hypothesized to be a factor in the development of Alzheimer's disease. We report the first quantitative study of glymphatic flow in man, combining intrathecal administration of gadobutrol with serial T1 mapping to produce contrast concentration maps up to 3 days postinjection, demonstrating performing a quantitative study using the techniques described feasibility and providing data on pharmacokinetics.

ABBREVIATION: AD = Alzheimer's disease

Protein aggregation is the pathologic signature of many neurodegenerative diseases, including Alzheimer's disease (AD).[1] The recently discovered glial lymphatic ("glymphatic") system[2] may play a critical role in protein removal, including soluble amyloid-β[3] and HPF-τ (Hyperphosphorylated-τ).[4] This perivascular glymphatic pathway drives exchange between CSF and interstitial fluid, and dysfunction may be a causal factor in the development of Alzheimer's disease.[5] In rodent models, glymphatic flow decreases with age,[6] increases during sleep,[7] and can be pharmacologically manipulated,[7] suggesting similar approaches for patients with AD.

Qualitative MR imaging using percentage signal enhancement on T1-weighted images has been reported in animal models[8] and humans.[9-12] However, the percentage signal change on a T1-weighted image with contrast concentration depends on the intrinsic T1 of each tissue, the corresponding change in $T2^*$, and the imaging parameters selected. To be able to apply pharmacokinetic models requires consistent determination of contrast concentrations across tissue types and concentrations. Here we use the combination of an intrathecal administration of a gadolinium-based contrast agent (gadobutrol) with quantitative MR imaging to provide maps of contrast concentration versus time, measuring glymphatic flow throughout the brain in a human volunteer at 3T.

MATERIALS AND METHODS

Patient History

A 55-year-old man referred for MR myelography was recruited for this Health Insurance Portability and Accountability Act–compliant, institutional review board (The Feinstein Institute for Medical Research)–approved study using an intrathecal injection of 0.5 mL of 1.0 mmol of gadobutrol. The patient gave written, informed consent.

Data Acquisition and Analysis

Quantitative T1-mapping data were acquired on a 3T Achieva TX MR imaging scanner (Philips Healthcare, Best, the Netherlands) with an 8-channel head coil using a multiple flip angle 3D spoiled gradient-echo sequence with TE/TR = 2.8/20 ms; flip angles = 2°, 5°, 10°, 20°, 40°; FOV = 240 × 228 × 120 mm^3; acquired resolution = 1.2 × 1.2 × 1.2 mm^3. Acquisition time was 3 minutes 47 seconds for each flip angle using a sensitivity encoding factor of 2, to give a total time of 24 minutes. Scans were acquired at baseline and at 9 further acquisitions during the first 10 hours (60, 210, 240, 270, 370, 450, 500, 560, and 620 minutes), followed by acquisitions at 26, 50, and 79 hours. The subject was not restricted but was asked to remain supine for as much as possible during the first 10 hours but then was allowed to move normally for the remaining time. He had a normal night's sleep before being scanned the final 3 times.

Data Analysis: Theory

The method is based on the nuclear MR steady-state signal equation,

Received August 22, 2018; accepted after revision November 13.

From the Department of Radiology (R.W.), University of Vermont, Burlington, Vermont; and Department of Radiology (J.M.S., L.W., X.Z., C.G.F.), Lenox Hill Hospital and Donald and Barbara Zucker School of Medicine at Hofstra/Northwell, East Garden City, New York.

This study was funded by the Foundation of the American Society of Neuroradiology Boerger Research Fund for Alzheimer's Disease and Neurocognitive Disorders.

Paper previously presented, in part, at: Annual Meeting of the American Society of Functional Neuroradiology, October 15–17, 2018; Coronado, California.

Please address correspondence to Christopher G. Filippi, MD, Lenox Hill Hospital and Donald and Barbara Zucker School of Medicine at Hofstra/Northwell, Department of Radiology, 100 E 77th Street, NY, NY 10075; e-mail: cfilippi@northwell.edu and sairaallapeikko@gmail.com

http://dx.doi.org/10.3174/ajnr.A5931

$$S_i = M_0 \sin \alpha_i \frac{1 - E_1}{1 - \cos \alpha_i E_1},$$

where $E_1 = \exp\left(\frac{-TR}{T_1}\right)$, S_i is the signal intensity for each flip angle α_i, and M_0 is a constant representing the equilibrium magnetization. This equation can be transformed to a linear form, from which the gradient E_1 and hence the tissue T_1 can be determined.[13]

The T_1 value is related to the contrast agent concentration by

$$\frac{1}{T_1} = \frac{1}{T_{10}} + r_1 C,$$

Where T_{10} is the native T_1 value of the tissue (s), and r_1 is the relaxivity of the contrast agent, assumed to be 5.1 l/mmol/s for gadobutrol.

Data Processing

Each volume was coregistered to the 20° flip angle acquisition from the first scan acquired before contrast injection using SPM12 (http://www.fil.ion.ucl.ac.uk/spm/software/spm12). T1 maps were generated using least squares fitting to the signal equation using custom Matlab (MathWorks, Natick, Massachusetts) scripts. The precontrast map provided the baseline T_1 values (T_{10}), enabling contrast concentration to be calculated at each subsequent time.

Brain segmentation was performed using SPM12 on the 20° flip angle acquisition from the first scan acquired before contrast injection, resulting in native space gray matter, white matter, and CSF components. Cortical gray matter masks were defined by the intersection of the gray matter mask and the corresponding regions of the Montreal Neurological Institute structural atlas transformed to native space. Juxtacortical white matter and CSF masks were defined by the intersection of their native tissue components with the cortical gray matter mask expanded by 3 mm using only voxels with >95% probability of being the target tissue.

RESULTS

The time course of contrast concentration during 79 hours postinjection is shown in Fig 1. Contrast arrived in the cisterna magna between 1 and 3 hours postinjection and covered the entire subarachnoid space at 8 hours. The subarachnoid CSF concentration peaked between 10 and 15 hours at approximately 0.5 mmol/L. Cortical enhancement measurable from 4 hours peaked between 10 and 26 hours, with a maximum concentration of approximately 0.1 mmol/L. The largest concentration was noted in the temporal lobes and insula in the first 10 hours. Cortical contrast remained at 50 hours with near-complete clearance at 79 hours. Depending on location, white matter concentration peaked between 26 and 50 hours.

Concentration-time curves were calculated for cortical gray matter and juxtacortical white matter (Fig 2). Biologic half-life of gadobutrol in the subarachnoid CSF, based on the washout curve, was approximately 12 hours. A 2-compartment model provided a good fit to the cortical contrast concentration curve.

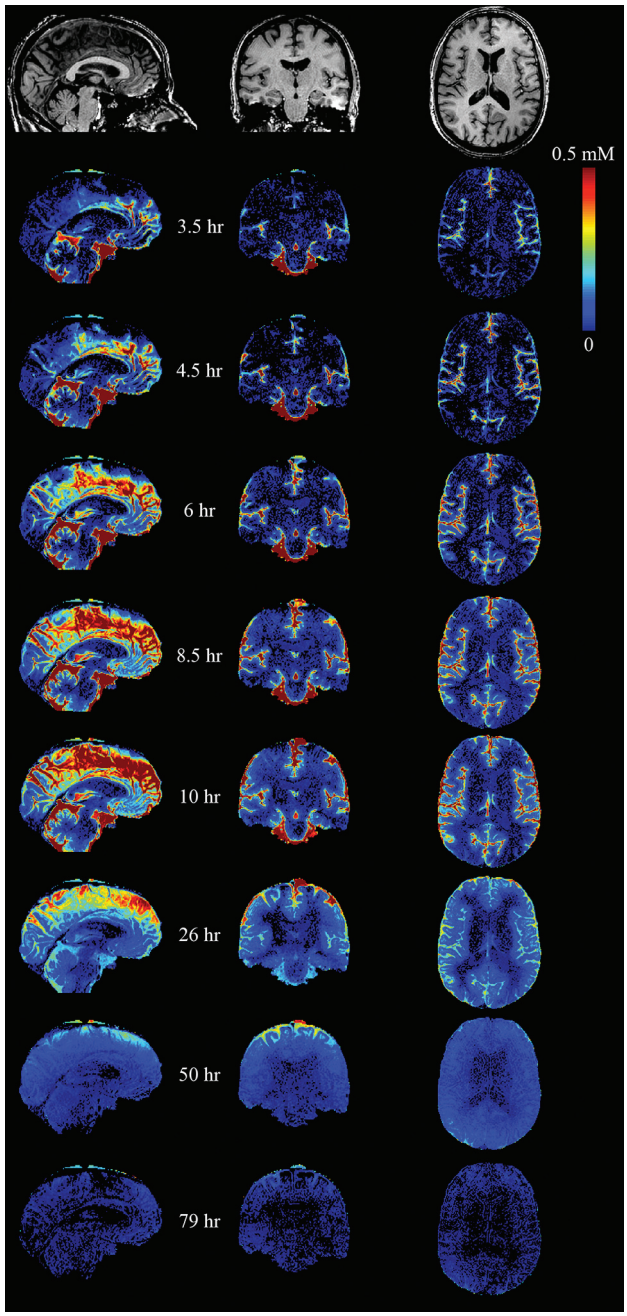

FIG 1. Quantitative maps of gadolinium tracer across time. The tracer arrived in the cisterna magna between 1 and 3.5 hours after intrathecal injection. Superior parts of the subarachnoid space enhance late, with clearance also delayed.

DISCUSSION

Most current literature on glymphatic flow is based on rodent models using highly invasive techniques. A few studies used MR imaging qualitatively to investigate glymphatic flow in rodents[8] and humans.[9-12] Our report improves on those studies by quantifying contrast concentration. We are only aware of a single study that has used similar quantification in rats at 9.4T.[14] Compared with rodents, contrast uptake and clearance are much slower in our subject but are still faster than would be expected due to only passive diffusion, which provides further evidence that intrathecal administration of drugs may provide access to the entire brain parenchyma.

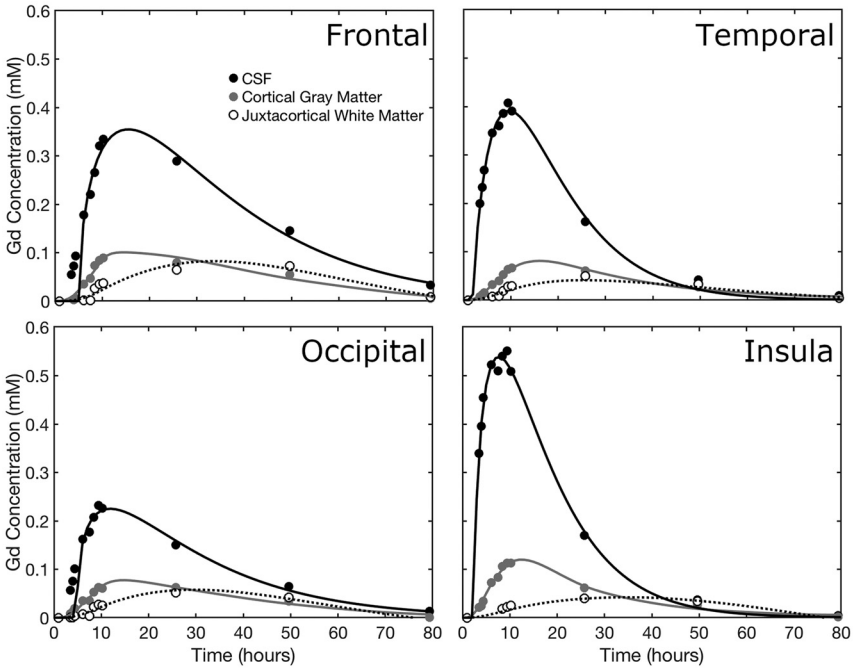

FIG 2. The time course of gadolinium concentration for the frontal, temporal, occipital, and parietal lobes. CSF concentration, cortical gray matter, and juxtacortical white matter curves are shown. Juxtacortical white matter is within 3 mm of the cortex. In each case, the CSF tracer concentration is fitted to a γ-variate distribution, while the tissue concentrations are fitted by 2-compartment pharmacokinetic models.

We observed minimal enhancement of the lateral ventricles at any time, suggesting that contrast entering the ventricular system is rapidly diluted.

Although only a single individual was imaged, the acquisition of serial quantitative data at many time points during 3 days represents a unique dataset. While cost and inconvenience to patients of an identical approach are prohibitive for routine use, our results suggest that an abbreviated protocol may suffice.

Regarding retention of gadolinium-based contrast agents, recent studies including long-term follow-up after intrathecal contrast injection have not identified adverse effects.[15,16] Gadolinium retention after intrathecal administration was not observed for gadobutrol at the same dose used in the current study.[11]

CONCLUSIONS

We have demonstrated the feasibility of using T1 mapping to quantify contrast concentration to analyze glymphatic flow in man, for which there is increasing interest in its use as a biomarker and potential therapeutic target in AD.

Disclosures: Richard Watts—*RELATED*: *Grant*: Foundation of the American Society of Neuroradiology Boerger Research Fund for Alzheimer's Disease and Neurocognitive Disorders.* Christopher G. Filippi—*RELATED*: *Grant*: Foundation of the American Society of Neuroradiology, *Comments*: Grant money was given by the Foundation of the American Society of Neuroradiology Boerger Fund to support this research study*; *UNRELATED*: *Consultancy*: Syntactx Inc, *Comments*: I read MR imaging examinations as part of clinical trials work. *Money paid to the institution.

REFERENCES

1. Ross CA, Poirier MA. **Protein aggregation and neurodegenerative disease.** *Nat Med* 2004;10(Suppl):S10–17 Medline
2. Iliff JJ, Wang M, Liao Y, et al. **A paravascular pathway facilitates CSF flow through the brain parenchyma and the clearance of interstitial solutes, including amyloid β.** *Sci Transl Med* 2012;4:147ra111 CrossRef Medline
3. Hawkes CA, Sullivan PM, Hands S, et al. **Disruption of arterial perivascular drainage of amyloid-β from the brains of mice expressing the human APOE ε4 allele.** *PLoS One* 2012;7:e41636 CrossRef Medline
4. Iliff JJ, Chen MJ, Plog BA, et al. **Impairment of glymphatic pathway function promotes tau pathology after traumatic brain injury.** *J Neurosci* 2014;34:16180–93 CrossRef Medline
5. Bakker EN, Bacskai BJ, Arbel-Ornath M, et al. **Lymphatic clearance of the brain: perivascular, paravascular and significance for neurodegenerative diseases.** *Cell Mol Neurobiol* 2016;36:181–94 CrossRef Medline
6. Hawkes CA, Hartig W, Kacza J, et al. **Perivascular drainage of solutes is impaired in the ageing mouse brain and in the presence of cerebral amyloid angiopathy.** *Acta Neuropathol* 2011;121:431–43 CrossRef Medline
7. Xie L, Kang H, Xu Q, et al. **Sleep drives metabolite clearance from the adult brain.** *Science* 2013;342:373–77 CrossRef Medline
8. Iliff JJ, Lee H, Yu M, et al. **Brain-wide pathway for waste clearance captured by contrast-enhanced MRI.** *J Clin Invest* 2013;123:1299–309 CrossRef Medline
9. Eide PK, Ringstad G. **MRI with intrathecal MRI gadolinium contrast medium administration: a possible method to assess glymphatic function in human brain.** *Acta Radiol Open* 2015;4:2058460115609635 CrossRef Medline
10. Eide PK, Ringstad G. **Delayed clearance of cerebrospinal fluid tracer from entorhinal cortex in idiopathic normal pressure hydrocephalus: a glymphatic magnetic resonance imaging study.** *J Cereb Blood Flow Metab* 2018;Feb 27:271678X18760974. [Epub ahead of print] CrossRef Medline
11. Ringstad G, Valnes LM, Dale AM, et al. **Brain-wide glymphatic enhancement and clearance in humans assessed with MRI.** *JCI Insight* 2018 Jul 12;3(13). [Epub ahead of print] CrossRef Medline
12. Ringstad G, Vatnehol SAS, Eide PK. **Glymphatic MRI in idiopathic normal pressure hydrocephalus.** *Brain* 2017;140:2691–705 CrossRef Medline
13. Cheng HL, Wright GA. **Rapid high-resolution T(1) mapping by variable flip angles: accurate and precise measurements in the pres-**

ence of radiofrequency field inhomogeneity. *Magnetic Reson Med* 2006;55:566–74 CrossRef Medline
14. Lee H, Mortensen K, Sanggaard S, et al. **Quantitative Gd-DOTA uptake from cerebrospinal fluid into rat brain using 3D VFA-SPGR at 9.4T.** *Magnetic Reson Med* 2018;79:1568–78 CrossRef Medline
15. Safriel Y, Ang R, Ali M. **Gadolinium use in spine pain management procedures for patients with contrast allergies: results in 527 procedures.** *Cardiovasc Intervent Radiol* 2008;31:325–31 CrossRef Medline
16. Nacar Dogan S, Kizilkilic O, Kocak B, et al. **Intrathecal gadolinium-enhanced MR cisternography in patients with otorhinorrhea: 10-year experience of a tertiary referral center.** *Neuroradiology* 2018;60:471–77 CrossRef Medline